Table I
Physical Properties of Fractions Obtained by Extracting with Boiling Solvents the Polymeric Products Obtained by Copolymerizing (*RS*)-3,7-Dimethyl-1-octene [(*RS*)-DMO] with (*S*)-3-Methyl-1-pentene [(*S*)-3MP][a]

	simultaneous addition of (*RS*)-DMO and (*S*)-3MP (3.8/1 molar ratio)			addition of (*RS*)-DMO to polymerizing (*S*)-3MP (2/1 molar ratio)		
fraction[b]	wt %	$[\alpha]^{25}_{D}$,[c] deg	D_{763}/D_{732}[d]	wt %	$[\alpha]^{25}_{D}$,[c] deg	D_{763}/D_{732}[d]
1	6.3	+6.0	n.d.	4.8	+12.0	n.d.
2	10.8	+41.3	0.50	8.3	+61.4	0.64
3	51.8	+64.5	0.60	60.4	+71.6	0.62
4	31.0	−20.4	0.32	26.5	+25.7	0.58

[a] Molar ratios α-olefins/Ti, Al(*i*-Bu)$_3$/Ti, and Al(*i*-Bu)$_3$/external base are 3600, 167, and 3, respectively; reaction temperature = 50 °C; solvent = *n*-heptane. [b] Extracted successively with acetone (1), ethyl acetate (2), diethyl ether (3), and cyclohexane (4). [c] In cyclohexane solution; l = 1 dm. [d] D_{763} and D_{732} are the optical densities of the IR bands related to poly(3MP) and poly(DMO), respectively; D_{763}/D_{732} is 13 for poly(3MP) and 0.11 for poly(DMO) (see ref 4).

Table II
Relative Polymerization Rate of the Two Antipodes of (*RS*)-3,7-Dimethyl-1-octene [(*RS*)-DMO] in the Presence of (*S*)-3-Methyl-1-pentene [(*S*)-3MP]

			nonpolymerized DMO		
run	(*RS*)-DMO/ (*S*)-3MP[a]	conv, %	enan purity	abs conf	k_S/k_R[b]
1 step	3.8	4.6	0.14	*R*	1.06
2 steps	2.0	9.1	1.20	*R*	1.27

[a] Overall (*RS*)-DMO/(*S*)-3MP molar ratio. [b] Relative polymerization rate of the two antipodes, calculated as $(100 + P_p)/(100 - P_p)$, where P_p is the enantiomeric purity of the polymerized DMO (see ref 4).

of (*S*)-3MP units [formed before addition of (*RS*)-DMO] attached to a block of random (*S*)-3MP/(*S*)-DMO copolymer (Scheme Ib). This block copolymer is expected to be less soluble than the analogous random copolymer obtained in the one-step experiment and thus could be not easily separated from the homopolymer of (*R*)-DMO. According to this hypothesis no substantial residue was found after cyclohexane extraction, indicating almost no formation of (*S*)-3MP homopolymer, which is more than 90% insoluble in this solvent.[8] Lack of (*S*)-3MP homopolymer suggests that most chains were living when (*RS*)-DMO was added. Furthermore, the optical rotation of the last fraction, as well as the content of (*S*)-3MP units, is lower than for the previous fractions as expected in the case of a substantially stereoselective process.

It must also be noted that in this latter experiment the recovered nonpolymerized DMO is optically active according again to a preferential polymerization of the *S* enantiomer, with an increase of the k_S/k_R ratio from 1.06 to 1.27 (Table II). Such higher stereoelectivity, which corresponds to an enantiomeric purity 6 times higher, cannot be simply explained by taking into account the larger (*S*)-3MP content (less than 2 times) and the use of (−)-menthyl benzoate [(−)-MtB] as external base. Indeed, (−)-MtB, employed because its high chemical purity allowed us to obtain a good activity with the sterically hindered olefins of the present investigation, is known to give an extremely low stereoelectivity.[9] It is likely that the chiral discrimination of the active sites is affected by the two-step addition either because centers with living (*S*)-3MP homopolymer are more stereoelective or because all *R* and *S* sites are affected by solvation by the optically active olefins.[10]

These preliminary results confirm nicely and simply the stereoselective character of the new generation high-activity Ziegler–Natta catalysts and indicate that the use of chiral monomers, one racemic and the other optically active, constitutes an informative approach for testing the capability of high-activity Ziegler–Natta catalysts to give block or stereoblock copolymers as well as of the monomer to affect the stereochemistry of active sites.

Acknowledgment. Partial support by the Ministry of Public Education is gratefully acknowledged.

Registry No. (±)-DMO, 13827-59-3; (*S*)-3MP, 5026-95-9; EtB, 93-89-0; PC, 106-44-5; MT, 99-75-2; ((*S*)-3MP((±)-DMO) (block copolymer), 105931-32-6; $MgCl_2$, 7786-30-3; $AlEt_o$, 97-93-8; $TiCl_4$, 7550-45-0.

References and Notes

(1) Pino, P.; Oschwald, A.; Ciardelli, F.; Carlini, C.; Chiellini, E. In *Coordination Polymerization. A Memorial to Karl Ziegler*; Chien, J. C. W., Ed.; Academic: New York, 1975; pp 25–72.
(2) Montagnoli, G.; Pini, D.; Lucherini, A.; Ciardelli, F.; Pino, P. *Macromolecules* **1969**, *2*, 684–686.
(3) Pino, P.; Fochi, G.; Oschwald, A.; Piccolo, O.; Mulhaupt, R.; Giannini, U. In *Coordination Polymerization*; Price, C. C., Vandenberg, E. J., Eds.; Plenum: New York, 1983; Pp 207–223.
(4) Ciardelli, F.; Carlini, C.; Montagnoli, G. *Macromolecules* **1969**, *2*, 296–301.
(5) Chien, J. C. W.; Wu, J. C.; Kuo, Chi-I. *J. Polym. Sci., Polym. Chem. Ed.* **1982**, *20*, 2019–2032.
(6) Ciardelli, F.; Montagnoli, G.; Pini, D.; Pieroni, O.; Carlini, C.; Benedetti, E. *Makromol. Chem.* **1971**, *147*, 53–68.
(7) Chien, J. C. W.; Kuo, Chi-I. *J. Polym. Sci. Polym. Chem. Ed.* **1986**, *24*, 1779–1818.
(8) Pino, P.; Ciardelli, F.: Lorenzi, G. P.; Montagnoli, G. *Makromol. Chem.* **1963**, *61*, 207–224.
(9) Ciardelli, F.; Carlini, C.; Altomare, A.; Menconi, F. *J. Chem. Soc., Chem. Commun.*, in press.
(10) Carlini, C.; Nocci, R.; Ciardelli, F. *J. Polym. Sci., Polym. Chem. Ed.* **1977**, *15*, 767–770.
(11) Dipartimento di Chimica e Chimica Industriale, Università di Pisa.
(12) Centro di Studio del CNR per le Macromolecole Stereordinate ed Otticamente Attive, Università di Pisa.
(13) Dipartimento di Chimica Industriale e dei Materiali, Università di Bologna.

C. Carlini,*[12,13] A. Altomare,[11] F. Menconi,[11] and F. Ciardelli*[11,12]

Dipartimento di Chimica e Chimica Industriale and Centro di Studio del CNR per le Macromolecole Stereordinate ed Otticamente Attive, Università di Pisa 56100 Pisa, Italy, and Dipartimento di Chimica Industriale e dei Materiali, Università di Bologna, Bologna, Italy

Received August 12, 1986

Time-Dependent Ginzburg–Landau Approach for Microphase-Separation Kinetics of Block Polymers

In this communication we present an approach to the interpretation of the qualitative basic phenomena underlying the time evolution of the order parameter of block polymers and mixtures of block polymers with themselves or homopolymers in the process of microphase separation, i.e., the phase transition from the disordered state to the

0024-9297/87/2220-0465$01.50/0

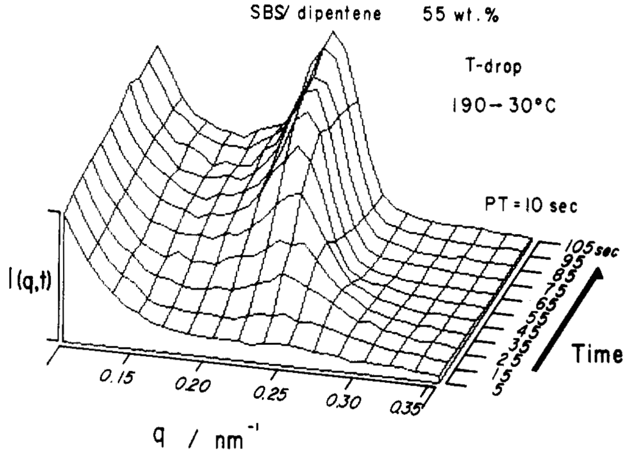

Figure 1. Isometric display of time-resolved SAXS profiles during the disorder–order transition of a 55 wt % SBS solution in dipentene. The temperature of the solution was rapidly dropped from 190 to 30 °C in about 10 s, the transition temperature T_r being 160 °C. PT is the time interval used to measure each SAXS profile. $q = (4\pi/\lambda)\sin(\theta/2)$, the scattering vector.

ordered state. We would like to present a proposal that a unique characteristic of wavenumber (q) dependence of the local chemical potential $\mu(q)$ of the block polymers (see eq 8) is a primary cause of their unique ordering dynamics, especially the dynamics at shallow quenches and in the early stage: the growth rate $R(q)$ has a maximum value at $q = q^* \sim 1/R_g$, the gyration radius of block polymers.

Dynamics in the phase transition of binary polymer mixtures is an important research topic in polymer physics and has stimulated extensive experimental and theoretical investigations in recent years.[1-13] However, much less attention has been focused on the study of the dynamics in block polymers, despite the fact that there exist interesting and rich physical phenomena concerning the molecular connectivity of the A and B polymers in A–B, A–B–A, and $-(\text{A–B})_n-$ block polymers. In a series of recent works the connectivity has been shown to have a significant effect on the concentration fluctuations of the A and B segments in both the ordered[14-17] and the disordered states[18-21,33,34] and to give the concentration fluctuations much different from those in the mixtures of polymer A and B.

Despite the increasing interest in the equilibrium aspects of the phase transition in block polymers, its dynamical studies are still in the embryonic stage. Only a few works[23-25] of a relatively preliminary nature exist on the microphase dissolution, i.e., the transition from the ordered state to the disordered state. Thus the kinetics of the ordering transition in block polymers is a completely new problem, and no theories have been presented so far. Here we propose the simplest time-dependent Ginzburg–Landau (TDGL)[26] approach to describe qualitatively the most important features in the ordering dynamics of block polymers. The same approach has been proposed to describe the early stage of the spinodal decomposition of mixtures.[2,7,22]

Figure 1 shows the typical time evolution behavior of small-angle X-ray scattering (SAXS) profiles after a temperature drop from 190 to 30 °C for 55 wt % SBS block polymer (polystyrene-*b*-polybutadiene-*b*-polystyrene block polymer) solution in dipentene. The specimen has a number-average molecular weight of 5.8×10^4 and weight fraction of polystyrene of 0.48. Its morphology is alternating lamellar microdomains in the ordered state in bulk or in neutral solvents. The solvent dipentene is neutrally good for both polystyrene (PS) and polybutadiene (PB) and is equally partitioned in the PS and PB microdomains in the ordered state,[27-29] acting simply as a diluent of the thermodynamic interaction parameter χ between the two polymers. Hence the solvent may not significantly alter the ordering mechanism of the bulk block polymers.

The solution has the order–disorder transition temperature $T_r = 160$ °C. Consequently 190 and 30 °C are well above and below T_r, respectively. The time evolution of the scattering during the transition was detected in real time by the time-resolved SAXS technique, each profile being consecutively recorded at a time interval of 10 s. The detailed experimental technique and results will be described elsewhere.[30]

Important observations in Figure 1 are as follows. A distinct scattering maximum appears shortly after the temperature drop. In the initial stage of the transition, the peak position $q_{\max}$ appears to have a nearly constant value, and the intensity at a given q exponentially increases with time t.[30] With a further increase of t, the scattering profile becomes sharp, and $q_{\max}$ slightly shifts toward smaller angles, reflecting a "shaping-up" process of the microdomains, i.e., a narrowing of the interfacial region and a stretching of the block chains normal to the interface in the microdomain space.[20b] The sharp scattering maximum at $t > 100$ s is due to the periodic microdomain structure of the SBS solution at 30 °C. The major interesting points to be considered are as follows:

(1) The wavenumber $q_{\text{m,block}}$ of the dominant Fourier component of the fluctuations is much larger than that, $q_{\text{m,blend}}$, for the early-stage spinodal decomposition of polymer mixtures.[4,10,11] Typically

$$q_{\text{m,block}} \simeq 0.23\ \text{nm}^{-1} \simeq \mathcal{O}(R_g^{-1}) \qquad (1)$$

$$q_{\text{m,block}}/q_{\text{m,blend}} \gtrsim \mathcal{O}(10) \qquad (2)$$

(2) In the early stage, the scattered intensity at a given q, $I(q,t)$, grows exponentially with time t

$$I(q,t) = I(q,0)\exp[2R(q)t] \quad \text{(early stage)} \qquad (3)$$

The points described above may be generally described by a phenomenological theory of TDGL[26]

$$\frac{\partial\psi(\mathbf{r},t)}{\partial t} = L_0\nabla^2\left[\frac{\delta\Delta F(r,t)}{\delta\psi(r,t)}\right] + f_r(\mathbf{r},t) \qquad (4)$$

where $\psi(\mathbf{r},t)$ is the conserved order parameter that describes spatial concentration fluctuations of one type of component, e.g., A at a given time t. The quantity L_0 is the Onsager kinetic coefficient, which is assumed to be a constant independent of $\mathbf{r}$, the assumption being valid for the initial stage of the phase transition. The quantity f_r is the random thermal force.[31] We take the q Fourier component for the nonlinear Langevin equation and assume $f_r = 0$ for simplification. Then

$$\frac{\partial\psi_q(\mathbf{r},t)}{\partial t} = L_0\nabla^2\left(\frac{\delta\Delta F}{\delta\psi}\right)_q \qquad (5)$$

where ΔF is the coarse-grained free energy functional of the block polymer systems. We found that Leibler's equation is quite appropriate for ΔF and is one of the best available equations at present.[18] Leibler derived the free energy functional as a power series of ψ

$$\Delta F = \tfrac{1}{2}\sum_q S_e(q)^{-1}|\psi_q|^2 + F_3 + F_4 + \ldots \qquad (6)$$

where F_n are the higher order terms, and $S_e(q)$ is given by, in the context of the random phase approximation (RPA)

$$S_e(q) = [S(q)/W(q) - 2\chi]^{-1} \sim I(q) \qquad (7)$$

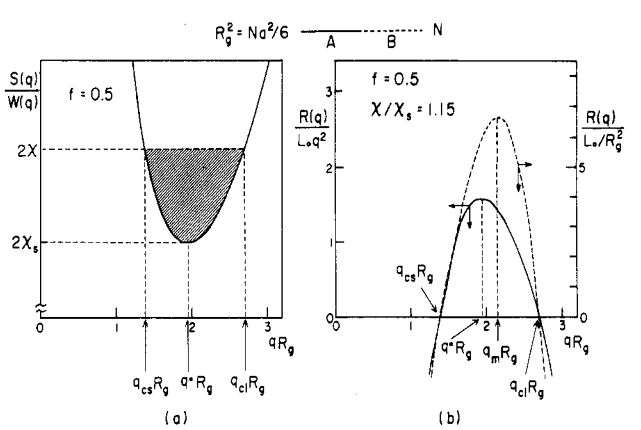

Figure 2. (a) $S(q)/W(q)$ and (b) $R(q)/(L_0q^2) = -S_e(q)^{-1}$ (the thermodynamic driving force) and $R(q)/(L_0/R_g^2)$ (the growth rate for the q Fourier component) for block polymers with a volume fraction of A equal to 0.5 and $\chi/\chi_s = 1.15$. R_g is the radius of gyration of the entire block chain of the A–B block polymers. χ_s is the thermodynamic interaction parameter between A and B at the spinodal point.

The function $S_e(q)$ is the Fourier transform of the density–density correlation function in the disordered state and hence is proportional to the scattering function $I(q)$. The detailed formula for $S_e(q)$ was given in Leibler's paper.[18] The local chemical potential $\mu(q)$ can be calculated from eq 6

$$\mu(q) = (\delta\Delta F/\delta\psi)_q = S_e(q)^{-1}\psi_q \tag{8}$$

We assume that the terms F_n ($n > 3$) are negligibly small compared with F_2 in eq 6. This *linearization approximation* may be good in the early stage of the microphase transition since $\psi_q(\mathbf{r},t)$ is small in that stage.

By combining eq 5, 6, and 8, one obtains

$$\frac{d\psi(q,t)}{dt} = L_0q^2[-S_e(q)^{-1}]\psi(q,t) \tag{9}$$

or

$$\psi(q,t) = \psi(q,0)\exp[R(q)t] \tag{10}$$

where

$$R(q) = L_0q^2[-S_e(q)^{-1}] \tag{11}$$

The time evolution of the scattered intensity is then given by

$$I(q,t) = \langle|\psi(q,t)|^2\rangle = I(q,0)\exp[2R(q)t] \tag{12}$$

Equations 10–12 predict the time evolutions of the order parameter and scattering function, both of which have an exponential growth behavior. The function $S_e(q)$ is positive in the single-phase region, and hence the fluctuations cannot grow since $R(q) < 0$. However, it becomes negative for a certain range of q in the two-phase region, and hence the fluctuations can grow since $R(q) > 0$. Equation 12 accounts for the experimental observation given by eq 3. The thermodynamic driving force for the growth of the order parameter $[-S_e(q)^{-1}]$ is given by calculating $S(q)/W(q)$ in eq 7 for the systems of one's interests. This thermodynamic part will give an important physical factor to predict the experimental observation given by eq 1, as will be clarified in the following discussion.

It should be noted that L_0 in eq 9 and 11 generally has a q dependence. This q dependence was calculated for the polymer mixture[6] but not for the block polymer. For the discussions presented in this communication we simply take L_0 to be a constant equal to the coefficient at the limit $q = 0$. Although the assumption should be thoroughly investigated theoretically in the future, it may be good enough for the ordering in the limit of *very shallow quench* and *in the early stage*.

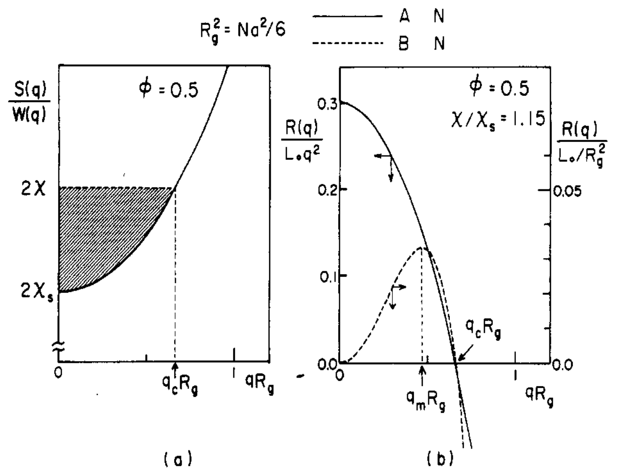

Figure 3. (a) $S(q)/W(q)$ and (b) $R(q)/(L_0q^2) = -S_e(q)^{-1}$ (the thermodynamic driving force) and $R(q)/(L_0/R_g^2)$ (the growth rate for the q Fourier component) for polymer blends with a volume fraction of A equal to 0.5, $\chi/\chi_s = 1.15$, and equal degrees of polymerization N for A and B. R_g is the radius of gyration of the polymers A and B (assumed to be identical).

Figure 2a shows the result of numerical calculations of the function $S(q)/W(q)$ plotted against qR_g ($R_g = Na^2/6$) for the A–B diblock polymer with a fraction of one constituent polymer A equal to 0.5 (N and a are the total degree of polymerization and the Kuhn statistical segment length of the A–B block polymer, respectively). At the spinodal point

$$2\chi_s = [S(q)/W(q)]_{q=q^*} \tag{13}$$

where q^* is the q value at which $S(q)/W(q)$ becomes a minimum. In the case when $2\chi > 2\chi_s$, the thermodynamic driving force for the growth of the fluctuation exists in the q region satisfying

$$q_{cs} < q < q_{cl} \tag{14}$$

and is given in Figure 2b for $\chi/\chi_s = 1.15$ (solid curve) where q_{cs} and q_{cl} are *the lower* and *upper bounds for the critical wavenumbers of the growing fluctuations*, respectively. The function $S(q)/W(q)$ becomes a minimum and hence $-S_e(q)^{-1} = R(q)/(L_0q^2)$ becomes a maximum at $q = q^*$. Figure 2b includes also the growth rate $R(q)/(L_0/R_g^2)$ as a function of qR_g (broken curve), clearly indicating that the maximum growth rate occurs at q_m

$$q_m \simeq q^* \sim 1/R_g \tag{15}$$

Thus the wavelength $2\pi/q_m$ or the wavenumber q_m of the dominant Fourier component of the growing fluctuations in the early stage is primarily determined by the Fourier component q^* with a maximum thermodynamic driving force, i.e., by the physical factor associated with the *molecular connectivity*. This accounts for the experimental observation given by eq 1. This is one of the big differences between the behavior of the block polymers and that of the polymer blends. In other words, an important difference exists in the fact that the block polymer has a *lower critical wavenumber* q_{cs}, which the polymer blends do not have.

Figure 3 shows $S(q)/W(q)$ (Figure 3a) and $R(q)/L_0q^2$ and $R(q)/(L_0/R_g^2)$ (Figure 3b) for polymer mixtures with an equal degree of polymerization and equal compositions for the polymers A and B ($\phi = 0.5$) ($\chi/\chi_s = 1.15$). In contrast to the block polymers, the polymer blends have a minimum value of $S(q)/W(q)$ and hence a maximum value of the thermodynamic driving force $R(q)/(L_0q^2)$ at $q = 0$ and only the upper bound of q_c[2,22]

$$q_c^2 = \tfrac{3}{2}(\epsilon/R_g^2), \qquad \epsilon = (\chi - \chi_s)/\chi_s \tag{16}$$

For the blends the critical wavenumber q_c, where the dynamics crossover between the growth and the dissolution, goes to zero with decreasing quench depth $(\chi - \chi_s)$, as is clear from Figure 3a, while for the block polymers q_c approaches $q^* \sim 1/R_g$, as is clear from Figure 2a; i.e.

$$\lim_{\epsilon \to 0} q_c = 0 \qquad \text{for blends}$$

$$\lim_{\epsilon \to 0} q_{cs} = \lim_{\epsilon \to 0} q_{cl} = q^* \qquad \text{for block polymers} \tag{17}$$

Thus in the shallow-quench limit, the q dependence of L_0 may not play an important role in the q dependence of $R(q)$ for block polymers. For the dominant Fourier component of the fluctuations q_m having a maximum growth rate $R(q_m)$

$$\lim_{\epsilon \to 0} q_m = 0 \qquad \text{for blends}$$

$$\lim_{\epsilon \to 0} q_m = q^* \sim 1/R_g \qquad \text{for block polymers} \tag{18}$$

This accounts for the experimental results as given by eq 1 and 2.

Equations 9–12 are valid for any binary polymer mixture, including A–B diblock polymers, A–B–A triblock polymers, and $-(\text{A–B})_n-$ multiblock polymers as well as mixtures of A and B, A–B and A, A–B, A, and B, A–B block polymers and A–B block polymers with different N and/or f (fraction of polymer A in the block polymer), etc., when appropriate functions are used[32] for $S(q)/W(q)$. A and B can be random copolymers of monomers A and B.[32] The block polymers can be star-shaped block polymers.[34]

The general equation (eq 9 or 11) for the growth of the fluctuation can be reduced to the formula derived by de Gennes[2] for the growth of the polymer blends as a special case. The de Gennes formula can be obtained at the small q regime and for the special case of binary blends with identical degree of polymerizations N and identical Kuhn statistical segment lengths a.

Acknowledgment. The author is grateful to professor T. Ohta and K. Kawasaki, Department of Physics, Kyushu University, Japan, Professor M. Muthkumar, Department of Polymer Science and Engineering, University of Massachusetts, and Professor M. Doi, Tokyo Metropolitan University, Tokyo, Japan, for helpful discussions.

Registry No. (PS)(PB) (block polymer), 106107-54-4.

References and Notes

(1) Nishi, T.; Wang, T. T.; Kwei, T. K. *Macromolecules* **1975**, *8*, 227.
(2) de Gennes, P.-G. *J. Chem. Phys.* **1980**, *72*, 4756.
(3) Nojima, S.; Tsutsui, K.; Nose, T. *Polym. J.* (*Tokyo*) **1982**, *14*, 225.
(4) Hashimoto, T.; Kumaki, S.; Kawai, H. *Macromolecules* **1983**, *16*, 641.
(5) Snyder, H. L.; Meakin, P.; Reich, S. *Macromolecules* **1983**, *16*, 757.
(6) Pincus, P. *J. Chem. Phys.* **1981**, *75*, 1966.
(7) Binder, K. *J. Chem. Phys.* **1983**, *79*, 6387.
(8) Nojima, S.; Ohyama, Y.; Yamaguchi, M.; Nose, T. *Polym. J.* (*Tokyo*) **1982**, *14*, 907.
(9) Snyder, H. L.; Meakin, P. *J. Chem. Phys.* **1983**, *79*, 5588.
(10) Sasaki, K.; Hashimoto, T. *Macromolecules* **1984**, *17*, 2818.
(11) Izumitani, T.; Hashimoto, T. *J. Chem. Phys.* **1985**, *83*, 3694.
(12) Inoue, T.; Ougizawa, T.; Yasuda, O.; Miyasaka, K. *Macromolecules* **1985**, *18*, 57.
(13) Russel, T. P.; Hadziioannou, G.; Warburton, W. K. *Macromolecules* **1985**, *18*, 78.
(14) Hashimoto, T.; Shibayama, M.; Kawai, H. *Macromolecules* **1980**, *13*, 1237. Hashimoto, T.; Fujimura, M.; Kawai, H. *Macromolecules* **1980**, *13*, 1660.
(15) Meier, D. J. *Prepr. Polym. Colloq., Soc. Polym. Sci. Jpn., Kyoto Jpn.* **1977**, 83.
(16) Helfand, E.; Wasserman, Z. R. *Macromolecules* **1976**, *19*, 879; **1978**, *11*, 960; **1980**, *13*, 994.
(17) Noolandi, J.; Hong, K. M. *Ferroelectrics* **1980**, *30*, 117.
(18) Leibler, L. *Macromolecules* **1980**, *13*, 1602.
(19) Roe, R. J.; Fishkis, M.; Chang, C. J. *Macromolecules* **1981**, *14*, 1091.
(20) (a) Mori, K.; Hasegawa, H.; Hashimoto, T. *Polym. J.* (*Tokyo*) **1985**, *17*, 799. (b) Hashimoto, T.; Shibayama, M.; Kawai, H. *Macromolecules* **1983**, *16*, 1093.
(21) Bates, F. S. *Macromolecules* **1985**, *18*, 525.
(22) Cahn, J. W. *J. Chem. Phys.* **1965**, *42*, 93.
(23) Hashimoto, T.; Tsukahara, Y.; Kawai, H. *J. Polym. Sci., Polym. Lett. Ed.* **1980**, *18*, 585; *Macromolecules* **1981**, *14*, 708.
(24) Hashimoto, T.; Kowsaka, K.; Shibayama, M.; Suehiro, S. *Macromolecules* **1986**, *19*, 750.
(25) Hashimoto, T.; Kowsaka, K.; Shibayama, M.; Kawai, H. *Macromolecules* **1986**, *19*, 754.
(26) See, for example: Gunton, J. D.; San Miguel, M.; Sahni, P. S. In *Phase Transitions and Critical Phenomena*; Domb, C., Lebowitz, J. L., Eds.; Academic: New York, 1983; Vol. 8.
(27) This fact was confirmed from the observation that the relative peak heights of the multiple-order SAXS maxima did not change when the SBS specimens were swelled with dipentene. The relative peak heights of the SAXS maxima are very sensitive to the volume fractions of the A and B microdomains.[28,29]
(28) Hashimoto, T.; Nagatoshi, K.; Todo, A.; Hasegawa, H.; Kawai, H. *Macromolecules* **1974**, *7*, 364.
(29) Shibayama, M.; Hashimoto, T. *Macromolecules* **1986**, *19*, 740.
(30) Sakurai, S.; Shibayama, M.; Kowsaka, K.; Hashimoto, T. *Macromolecules*, to be submitted.
(31) Cook, H. E. *Acta Metall.* **1970**, *18*, 297.
(32) The functional form for $S(q)/W(q)$ for some of the systems will be given elsewhere.[33]
(33) Mori, K.; Tanaka, H.; Hashimoto, T. *Macromolecules*, in press.
(34) Olvera de la Cruz, M.; Sanchez, I. *Macromolecules* **1986**, *19*, 2501.

Takeji Hashimoto
Department of Polymer Chemistry, Faculty of Engineering
Kyoto University, Kyoto 606, Japan

Received August 7, 1986